Collective Paths Connecting the Oblate and Prolate Shapes in ^{68}Se and ^{72}Kr Suggested by the Adiabatic Self-Consistent Collective Coordinate Method

Masato KOBAYASI,[1] Takashi NAKATSUKASA,[2] Masayuki MATSUO[3] and Kenichi MATSUYANAGI[1]

[1]*Department of Physics, Graduate School of Science, Kyoto University, Kyoto 606-8502, Japan*
[2]*Institute of Physics and Center for Computational Science, University of Tsukuba, Tsukuba 305-8571, Japan*
[3]*Graduate School of Science and Technology, Niigata University, Niigata 950-2181, Japan*

By means of the adiabatic self-consistent collective coordinate method and the pairing-plus-quadrupole interaction, we have for the first time obtained a self-consistent collective path connecting the oblate and prolate local minima in ^{68}Se and ^{72}Kr. This self-consistent collective path is found to run approximately along the valley connecting the oblate and prolate local minima in the collective potential energy landscape. The result of this calculation clearly indicates the importance of triaxial deformation dynamics in oblate-prolate shape coexistence phenomena.

§1. Introduction

The microscopic description of large amplitude collective motion in nuclei is a long-standing fundamental subject of nuclear structure physics.[1)–5)] In spite of the steady development of various theoretical concepts and mathematical formulations, the application of microscopic many-body theory to actual nuclear phenomena still remains a challenging task.[6)–33)] Shape coexistence phenomena are typical examples of large amplitude collective motion in nuclei, and both experimental and theoretical investigations of such phenomena are currently being carried out.[34)–57)] We are particularly interested in the recent discovery of two coexisting rotational bands in ^{68}Se and ^{72}Kr, which are associated with oblate and prolate intrinsic shapes.[41),42)] Clearly, these data strongly call for further development of a theory that is able to describe them and revise our understanding of nuclear structure. From the viewpoint of the microscopic mean-field theory, the coexistence of different shapes implies that different solutions of the Hartree-Fock-Bogoliubov (HFB) equations (local minima in the deformation energy surface) appear in the same energy region and that the nucleus exhibits large amplitude collective motion connecting these different equilibrium points. The identities and mixings of these different shapes are determined by the dynamics of such collective motion.

On the basis of the time-dependent Hartree-Fock (TDHF) theory, the self-consistent collective coordinate (SCC) method was proposed as a microscopic theory of such large amplitude collective motion.[12)] This method was extended to the case of time-dependent HFB (TDHFB) including pairing correlations,[23)] and it has been successfully applied to various kinds of anharmonic vibration and high-spin rotational phenomena.[58)–69)] In order to apply this method to shape coexistence phenomena, however, we need to further develop the theory, because the existing method of solving the basic equations of the SCC method, called the η-expansion method,[12)]

assumes a single local minima, whereas several local minima of the potential energy surface compete in these systems. Some years ago, we proposed a new method of describing such large-amplitude collective motion, called the adiabatic self-consistent collective coordinate (ASCC) method.[70] This method provides a practical scheme for solving the basic equations of the SCC method[12] using an expansion in terms of the collective momentum. It does not assume a single local minimum, and therefore it is believed to be suitable for the description of shape coexistence phenomena. The ASCC method inherits the major advantages of the adiabatic TDHF (ATDHF) methods and, in addition, enables us to include pairing correlations self-consistently. In this method, the spurious number fluctuation modes are automatically decoupled from the physical modes within the self-consistent framework of the TDHFB theory. This will certainly be a great advantage when the method is applied to realistic nuclear problems. To examine the feasibility of the ASCC method, in Ref. 71), we applied it to an exactly solvable model called the multi-$O(4)$ model,[72)–75)] which is a simplified version of the pairing-plus-quadrupole (P+Q) interaction model.[76)–78)] It was shown that this method yields a faithful description of tunneling motion through a barrier between prolate and oblate local minima in the collective potential.[71)]

In this paper, we report on our first application of the ASCC method to the P+Q interaction model. The major task here is to develop a practical procedure for solving the basic equations of the ASCC method in order to obtain a self-consistent collective path. We investigate, as typical examples, the oblate-prolate shape coexistence phenomena in ^{68}Se and ^{72}Kr,[41),42)] and we find that the self-consistent collective paths run approximately along the valley connecting the oblate and prolate local minima in the collective potential energy landscape. To the best of our knowledge, this is the first time that, starting from the microscopic P+Q Hamiltonian, the collective paths have been fully self-consistently obtained for realistic situations, although a similar approach to the study of large amplitude collective motion was recently employed by Almehed and Walet.[79),80)]

This paper is organized as follows. In §2, the basic equations of the ASCC method are summarized. In §3, we present a concrete formulation of the ASCC method for the case of the P+Q Hamiltonian. In §4, an algorithm to solve the basic equations of the ASCC method is discussed. In §5, we present the results of numerical calculations for the oblate-prolate shape coexistence phenomena in ^{68}Se and ^{72}Kr. Concluding remarks are given in §6.

A preliminary version of this work was reported previously in this journal.[81)]

§2. Basic equations of the ASCC method

In this section, we summarize the basic equations of the ASCC method.[70)] The basic assumption of our approach is that large-amplitude collective motion can be described by a set of time-dependent HFB state vectors $|\phi(q,p,\varphi,N)\rangle$ parameterized by a single collective coordinate q, the collective momentum p conjugate to q, the particle number N and the gauge angle φ conjugate to N. Then, the state vectors can be written in the following form:

$$|\phi(q,p,\varphi,N)\rangle = e^{-i\varphi\hat{N}}\,|\phi(q,p,N)\rangle = e^{-i\varphi\hat{N}}e^{ip\hat{Q}(q)}|\phi(q)\rangle. \tag{2·1}$$

Carrying out an expansion with respect to p and requiring that the time-dependent variational principle be satisfied up to second order in p, we obtain the following set of equations to determine $|\phi(q)\rangle$, the infinitesimal generator $\hat{Q}(q)$, and its canonical

conjugate $\hat{P}(q)$. First, we have *the HFB equation in the moving frame*, given by

$$\delta \langle\phi(q)| \hat{H}_M(q) |\phi(q)\rangle = 0, \tag{2·2}$$

where

$$\hat{H}_M(q) = \hat{H} - \lambda(q)\hat{N} - \frac{\partial V}{\partial q}\hat{Q}(q) \tag{2·3}$$

represents the Hamiltonian in the moving frame. Then, we have *the local harmonic equations in the moving frame*,

$$\delta \langle\phi(q)| [\hat{H}_M(q), \hat{Q}(q)] - \frac{1}{i}B(q)\hat{P}(q) |\phi(q)\rangle = 0, \tag{2·4}$$

$$\delta \langle\phi(q)| [\hat{H}_M(q), \frac{1}{i}\hat{P}(q)] - C(q)\hat{Q}(q) - \frac{1}{2B(q)}[[\hat{H}_M(q), (\hat{H} - \lambda(q)\hat{N})_A], \hat{Q}(q)] - \frac{\partial \lambda}{\partial q}\hat{N} |\phi(q)\rangle = 0, \tag{2·5}$$

where

$$B(q) = - \langle\phi(q)| [[\hat{H}, \hat{Q}(q)], \hat{Q}(q)] |\phi(q)\rangle \tag{2·6}$$

represents the inverse mass,

$$C(q) = \frac{\partial^2 V}{\partial q^2} + \frac{1}{2B(q)}\frac{\partial B}{\partial q}\frac{\partial V}{\partial q} \tag{2·7}$$

the local stiffness, and $(\hat{H} - \lambda\hat{N})_A$ denotes the two-quasiparticle creation and annihilation parts of $(\hat{H} - \lambda\hat{N})$.

The infinitesimal generators, $\hat{Q}(q)$ and $\hat{P}(q)$, satisfy *the canonical variable condition*:

$$\langle\phi(q)| [\hat{Q}(q), \hat{P}(q)] |\phi(q)\rangle = i. \tag{2·8}$$

Once $|\phi(q)\rangle$ and the infinitesimal generators are determined for every value of q, we obtain the collective Hamiltonian $\mathcal{H}(q,p) = \frac{1}{2}B(q)p^2 + V(q)$ with the collective potential $V(q) = \langle\phi(q)| \hat{H} |\phi(q)\rangle$.

In the above equations, no distinction is made between protons and neutrons for simplicity in the notation. In the actual calculations described below, however, we explicitly treat the neutron number N and the proton number Z separately.

§3. Application of the ASCC method to the P+Q model

3.1. *The P+Q Hamiltonian and signature quantum number*

Let us start with the well-known P+Q Hamiltonian,[76)–78)]

$$\hat{H} = \sum_k \epsilon_k c_k^\dagger c_k - \sum_\tau \frac{G_\tau}{2}\Big(A_\tau^\dagger A_\tau + A_\tau A_\tau^\dagger\Big) - \frac{\chi}{2}\sum_{K=-2}^{2} D_{2K}^\dagger D_{2K}, \tag{3·1}$$

where

$$A_\tau^\dagger = {\sum_{k\in\tau}}' c_k^\dagger c_{\tilde{k}}^\dagger, \quad A_\tau = {\sum_{k\in\tau}}' c_{\tilde{k}} c_k,$$
$$D_{2K} = \sum_{\tau=n,p}\sum_{kl\in\tau} D_{2K}^{(\tau)}(kl) c_k^\dagger c_l. \tag{3·2}$$

Here, we have $D_{2K}^{(\tau)}(kl) = \alpha_\tau^2 \langle k| r^2 Y_{2K} |l\rangle$, G_τ and χ denote the pairing and quadrupole force strengths, respectively, and $c_k^\dagger$ and c_k are the nucleon creation and annihilation operators in the single-particle state k, while $c_{\tilde{k}}^\dagger$ and $c_{\tilde{k}}$ denote those in the time-reversed state of k. The index τ indicates protons (with $\tau = p$) and neutrons (with $\tau = n$). Although it is not explicitly mentioned below, it should be kept in mind that the single-particle index k actually includes the index τ. The notation Σ' in the pair operators, $A_\tau^\dagger$ and A_τ, represents a sum over the pairs $(k, \tilde{k})$. The factors $\alpha_n = (2Z/A)^{2/3}$ and $\alpha_p = (2N/A)^{2/3}$, multiplying the quadrupole matrix elements, yield equivalent root-mean-square radii for protons and neutrons. Following Baranger and Kumar,[77] we take into account two major shells as the model space, and we multiply the quadrupole matrix elements $D_{2K}^{(\tau)}(kl)$ of the upper harmonic-oscillator shell by the reduction factor $\zeta = (N_L + 3/2)/(N_L + 5/2)$, N_L being the total number of oscillator quanta of the lower shell. Following the conventional prescription of the P+Q interaction,[76)–78)] we ignore the exchange (Fock) terms. In other words, we employ the Hartree-Bogoliubov (HB) approximation throughout this paper.

We introduce the following notations:

$$\begin{aligned} \hat{F}_s^{(\pm)} &\equiv \frac{1}{2}(\hat{F}_s \pm \hat{F}_s^\dagger), \\ \hat{F}_s^{(\pm)} &\equiv \{A_n^{(\pm)}, A_p^{(\pm)}, D_{20}^{(\pm)}, D_{21}^{(\pm)}, D_{22}^{(\pm)}\}. \qquad (s = 1-5) \end{aligned} \tag{3·3}$$

We then write the P+Q Hamiltonian in the form

$$\hat{H} = \sum_k \epsilon_k c_k^\dagger c_k - \sum_{s=1}^{5} \frac{\kappa_s}{2} \hat{F}_s^{(+)} \hat{F}_s^{(+)} + \sum_{s=1}^{5} \frac{\kappa_s}{2} \hat{F}_s^{(-)} \hat{F}_s^{(-)}, \tag{3·4}$$

where $\kappa_s = \{2G_n, 2G_p, \chi, 2\chi, 2\chi\}$ for $s = 1-5$. Our Hamiltonian is invariant with respect to a rotation by π about the x axis. The symmetry quantum number associated with it is called the signature, $r = e^{-i\pi\alpha}$. To exploit the signature symmetry, it is convenient to use nucleon operators with definite signatures defined by

$$\begin{aligned} d_k &\equiv \frac{1}{\sqrt{2}}(c_k + c_{\tilde{k}}), \qquad r = -i \ (\alpha = 1/2), \\ d_{\bar{k}} &\equiv \frac{1}{\sqrt{2}}(c_{\tilde{k}} - c_k), \qquad r = +i \ (\alpha = -1/2), \end{aligned} \tag{3·5}$$

and their Hermite conjugates, $d_k^\dagger$ and $d_{\bar{k}}^\dagger$. The operators $\hat{F}_s^{(\pm)}$ are then classified according to the signature quantum numbers, $r = \pm 1$ $(\alpha = 0, 1)$, as

$$\begin{aligned} \{A_n^{(\pm)}, A_p^{(\pm)}, D_{20}^{(+)}, D_{21}^{(-)}, D_{22}^{(+)}\}, \qquad (r = +1) \\ \{D_{21}^{(+)}, D_{22}^{(-)}\}, \qquad (r = -1) \end{aligned} \tag{3·6}$$

Note that $D_{20}^{(-)} = 0$. The HB local minima corresponding to the oblate and prolate equilibrium shapes possess positive signature, $r = +1 (\alpha = 0)$. Therefore, the operators $\hat{Q}(q)$ and $\hat{P}(q)$, generating large amplitude collective motion associated with these shapes, also possess positive signature. In other words, the negative signature degrees of freedom are exactly decoupled from the large amplitude collective motion

of interest, and hence we can ignore them. Also, it is readily confirmed that the $K = 1$ components associated with the quadrupole operator $\hat{D}_{21}^{(-)}$ exactly decouple from the $K = 0$ and 2 components in the local harmonic equations, (2.2) and (2.4). As is well known, they are associated with the collective rotational motion, and the large amplitude shape vibrational motion under consideration is exactly decoupled from them in the present framework. We note, however, that it is possible, with a rather straightforward extension, to formulate the ASCC method in a rotating frame of reference. By means of such an extension, we are able to take into account the coupling effects between the two kinds of large amplitude collective motion. It is certainly a very interesting subject to study how the properties of the large-amplitude shape vibrational motion change as a function of the angular momentum, but such an investigation is beyond the scope of this paper. We note, however, that an attempt to treat this subject was recently made by Almehed and Walet.[80)]

Thus, only the components $\{A_n^{(\pm)}, A_p^{(\pm)}, D_{20}^{(+)}, D_{22}^{(+)}\}$ are pertinent to the shape coexistence dynamics of interest presently. They all belong to the positive signature sector, and we are able to adopt a phase convention with which their single-particle matrix elements are real. In the following, we assume that this is the case.

3.2. *Quasiparticle-random-phase approximation (QRPA) at the HB local minima*

As discussed in the introduction, shape coexistence phenomena imply the existence of several local minima in the deformation energy surface, which are solutions of the HB equations. Let us choose one of them and write it $|\phi_0\rangle$. The HB equation is given by

$$\delta\langle\phi_0|\hat{H} - \sum_\tau \lambda_\tau \hat{N}_\tau|\phi_0\rangle = 0, \tag{3·7}$$

where λ_τ represents the chemical potentials for protons ($\tau = p$) and neutrons ($\tau = n$). The quasiparticle creation and annihilation operators, $a_\mu^\dagger$ and a_μ, associated with the HB local minimum are defined by $a_\mu|\phi_0\rangle = 0$. Similar equations hold for their signature partners, $\bar{\mu}$. They are introduced through the Bogoliubov transformations,

$$\begin{pmatrix} a_\mu^\dagger \\ a_{\bar{\mu}} \end{pmatrix} = \sum_k \begin{pmatrix} U_{\mu k} & V_{\mu \bar{k}} \\ V_{\bar{\mu} k} & U_{\bar{\mu}\bar{k}} \end{pmatrix} \begin{pmatrix} d_k^\dagger \\ d_{\bar{k}} \end{pmatrix}, \tag{3·8}$$

and their Hermite conjugate equations. (Here and hereafter, we do not mix protons and neutrons in these transformations.) In terms of the two quasiparticle creation and annihilation operators,

$$\boldsymbol{A}_{\mu\bar{\nu}}^\dagger \equiv a_\mu^\dagger a_{\bar{\nu}}^\dagger, \quad \boldsymbol{A}_{\mu\bar{\nu}} \equiv a_{\bar{\nu}} a_\mu, \tag{3·9}$$

the RPA normal coordinates and momenta describing small amplitude vibrations about the HB local minimum $|\phi_0\rangle$ are written

$$\hat{Q}_\rho = \sum_{\mu\bar{\nu}} Q_{\mu\bar{\nu}}^\rho (\boldsymbol{A}_{\mu\bar{\nu}}^\dagger + \boldsymbol{A}_{\mu\bar{\nu}}), \tag{3·10}$$

$$\hat{P}_\rho = i \sum_{\mu\bar{\nu}} P_{\mu\bar{\nu}}^\rho (\boldsymbol{A}_{\mu\bar{\nu}}^\dagger - \boldsymbol{A}_{\mu\bar{\nu}}), \tag{3·11}$$

where the sum is taken over the proton and neutron quasiparticle pairs ($\mu\bar{\nu}$), and ρ labels the QRPA modes. The amplitudes $Q_{\mu\nu}^\rho$ and $P_{\mu\nu}^\rho$ are determined by the QRPA

equations of motion,

$$\delta \langle\phi_0| [\hat{H} - \sum_\tau \lambda_\tau \hat{N}_\tau,\ \hat{Q}_\rho] - \frac{1}{i} B_\rho \hat{P}_\rho |\phi_0\rangle = 0, \tag{3·12}$$

$$\delta \langle\phi_0| [\hat{H} - \sum_\tau \lambda_\tau \hat{N}_\tau,\ \frac{1}{i}\hat{P}_\rho] - C_\rho \hat{Q}_\rho |\phi_0\rangle = 0, \tag{3·13}$$

and the orthonormalization condition $\langle\phi_0| [\hat{Q}_\rho, \hat{P}_{\rho'}] |\phi_0\rangle = i\delta_{\rho,\rho'}$.

3.3. *The HB equation and the quasiparticles in the moving frame*

For the P+Q Hamiltonian, the HB equation (2·2) determining the state vector $|\phi(q)\rangle$ away from the local minimum reduces to

$$\delta \langle\phi(q)| \hat{h}_M(q) |\phi(q)\rangle = 0, \tag{3·14}$$

where $\hat{h}_M(q)$ is the mean-field Hamiltonian in the moving frame,

$$\hat{h}_M(q) = \hat{h}(q) - \sum_\tau \lambda_\tau(q) \hat{N}_\tau - \frac{\partial V}{\partial q} \hat{Q}(q), \tag{3·15}$$

$$\hat{h}(q) = \sum_k \epsilon_k (d_k^\dagger d_k + d_{\bar{k}}^\dagger d_{\bar{k}}) - \sum_s \kappa_s \hat{F}_s^{(+)} \langle\phi(q)| \hat{F}_s^{(+)} |\phi(q)\rangle . \tag{3·16}$$

The state vector $|\phi(q)\rangle$ can be written in terms of a unitary transformation of $|\phi_0\rangle$:

$$|\phi(q)\rangle = e^{\hat{\theta}(q)} |\phi_0\rangle ,$$
$$\hat{\theta}(q) \equiv \sum_{\mu\bar{\nu}} \theta_{\mu\bar{\nu}}(q) \Big(\boldsymbol{A}^\dagger_{\mu\bar{\nu}} - \boldsymbol{A}_{\mu\bar{\nu}} \Big). \tag{3·17}$$

Here, the sum is taken over the proton and neutron quasiparticle pairs $(\mu\bar{\nu})$. The quasiparticle creation and annihilation operators, $a^\dagger_\mu(q)$ and $a_\mu(q)$, associated with the state $|\phi(q)\rangle$, which satisfy the condition $a_\mu(q)|\phi(q)\rangle = 0$, are written

$$a^\dagger_\mu(q) \equiv e^{\hat{\theta}}(q) a^\dagger_\mu e^{-\hat{\theta}(q)} = \sum_\nu \Big(U_{\mu\nu}(q) a^\dagger_\nu + V_{\mu\bar{\nu}}(q) a_{\bar{\nu}} \Big),$$
$$a_{\bar{\mu}}(q) \equiv e^{\hat{\theta}}(q) a_{\bar{\mu}} e^{-\hat{\theta}(q)} = \sum_\nu \Big(V_{\bar{\mu}\nu}(q) a^\dagger_\nu + U_{\bar{\mu}\bar{\nu}}(q) a_{\bar{\nu}} \Big), \tag{3·18}$$

where

$$\begin{pmatrix} U_{\mu\nu}(q) & V_{\mu\bar{\nu}}(q) \\ V_{\bar{\mu}\nu}(q) & U_{\bar{\mu}\bar{\nu}}(q) \end{pmatrix} = \begin{pmatrix} \cos(\sqrt{\theta\theta^T}) & -\theta \dfrac{\sin(\sqrt{\theta^T\theta})}{\sqrt{\theta^T\theta}} \\ \theta^T \dfrac{\sin(\theta\theta^T)}{\sqrt{\theta\theta^T}} & \cos(\sqrt{\theta^T\theta}). \end{pmatrix} \tag{3·19}$$

Here, θ on the r.h.s. represents the matrix composed of $\theta_{\mu\nu}(q)$, and it is understood that its elements corresponding to those on the l.h.s. should be taken.

In terms of the quasiparticle operators defined above, the mean-field Hamiltonian in the moving frame $\hat{h}_M(q)$, the neutron and proton number operators $\hat{N}_\tau$, and

the pairing and quadrupole operators $\hat{F}_s^{(\pm)}$ are written in the following forms:

$$\hat{h}_M(q) = \langle\phi(q)|\,\hat{h}_M(q)\,|\phi(q)\rangle + \sum_\mu E_\mu(q)\Big(\boldsymbol{B}_{\mu\mu}(q) + \boldsymbol{B}_{\bar{\mu}\bar{\mu}}(q)\Big), \tag{3·20}$$

$$\begin{aligned}\hat{N}_\tau = \langle\phi(q)|\,\hat{N}_\tau\,|\phi(q)\rangle &+ \sum_\mu N_\tau(\mu)\Big(\boldsymbol{A}^\dagger_{\mu\bar{\mu}}(q) + \boldsymbol{A}_{\mu\bar{\mu}}(q)\Big)\\ &+ \sum_\mu N_{B,\tau}(\mu)\Big(\boldsymbol{B}_{\mu\mu}(q) + \boldsymbol{B}_{\bar{\mu}\bar{\mu}}(q)\Big),\end{aligned} \tag{3·21}$$

$$\begin{aligned}\hat{F}_s^{(\pm)} = \langle\phi(q)|\,\hat{F}_s^{(\pm)}\,|\phi(q)\rangle &+ \sum_{\mu\bar{\nu}} F_s^{(\pm)}(\mu\bar{\nu})\Big(\boldsymbol{A}^\dagger_{\mu\bar{\nu}}(q) \pm \boldsymbol{A}_{\mu\bar{\nu}}(q)\Big)\\ &+ \sum_{\mu\nu} F_{B,s}^{(\pm)}(\mu\nu)\Big(\boldsymbol{B}_{\mu\nu}(q) + \boldsymbol{B}_{\bar{\mu}\bar{\nu}}(q)\Big),\end{aligned} \tag{3·22}$$

where

$$\boldsymbol{A}^\dagger_{\mu\bar{\nu}}(q) \equiv a^\dagger_\mu(q)a^\dagger_{\bar{\nu}}(q), \quad \boldsymbol{A}_{\mu\bar{\nu}}(q) \equiv a_{\bar{\nu}}(q)a_\mu(q), \quad \boldsymbol{B}_{\mu\nu}(q) \equiv a^\dagger_\mu(q)a_\nu(q). \tag{3·23}$$

Note that $E_{\bar{\mu}}(q) = E_\mu(q)$ and also that the equalities $F_{B,s}^{(\pm)}(\bar{\mu}\bar{\nu}) = F_{B,s}^{(\pm)}(\mu\nu)$ hold for the operators under consideration. Explicit expressions for the expectation values and the quasiparticle matrix elements appearing in the above equations are given in Appendix A.

3.4. *Local harmonic equations in the moving frame*

We can represent the infinitesimal generators $\hat{Q}(q)$ and $\hat{P}(q)$ in terms of $\boldsymbol{A}^\dagger_{\mu\bar{\nu}}(q)$ and $\boldsymbol{A}_{\mu\bar{\nu}}(q)$ as

$$\hat{Q}(q) = \sum_{\mu\bar{\nu}} Q_{\mu\bar{\nu}}(q)\Big(\boldsymbol{A}^\dagger_{\mu\bar{\nu}}(q) + \boldsymbol{A}_{\mu\bar{\nu}}(q)\Big), \tag{3·24}$$

$$\hat{P}(q) = i\sum_{\mu\bar{\nu}} P_{\mu\bar{\nu}}(q)\Big(\boldsymbol{A}^\dagger_{\mu\bar{\nu}}(q) - \boldsymbol{A}_{\mu\bar{\nu}}(q)\Big), \tag{3·25}$$

where the sum is taken over the proton and neutron quasiparticle pairs $(\mu\bar{\nu})$. For the P+Q Hamiltonian, the local harmonic equations, (2·4) and (2·5), in the moving frame reduce to

$$\delta\,\langle\phi(q)|\,[\hat{h}_M(q), \hat{Q}(q)] - \sum_s f^{(-)}_{Q,s}\hat{F}^{(-)}_s - \frac{1}{i}B(q)\hat{P}(q)\,|\phi(q)\rangle = 0, \tag{3·26}$$

$$\begin{aligned}\delta\,\langle\phi(q)|\,\Big[\hat{h}_M(q)\ ,\ \frac{1}{i}B(q)\hat{P}(q)\Big] - \sum_s f^{(+)}_{P,s}\hat{F}^{(+)}_s - B(q)C(q)\hat{Q}(q) - \sum_s f^{(+)}_{R,s}\hat{F}^{(+)}_s\\ + \sum_s f^{(-)}_{Q,s}\hat{R}^{(-)}_s - \sum_\tau f_{N,\tau}\hat{N}_\tau\,|\phi(q)\rangle = 0,\end{aligned} \tag{3·27}$$

where the quantities $f^{(-)}_{Q,s}$, etc., are given by

$$f^{(-)}_{Q,s} \equiv -\kappa_s\,\langle\phi(q)|\,[\hat{F}^{(-)}_s, \hat{Q}(q)]\,|\phi(q)\rangle = 2\kappa_s(F^{(-)}_s, Q(q)), \tag{3·28}$$

$$f^{(+)}_{P,s} \equiv \kappa_s\,\langle\phi(q)|\,\Big[\hat{F}^{(+)}_s, \frac{1}{i}B(q)\hat{P}(q)\Big]\,|\phi(q)\rangle = 2\kappa_s B(q)(F^{(+)}_s, P(q)), \tag{3·29}$$

$$f^{(+)}_{R,s} \equiv -\frac{1}{2}\kappa_s \langle\phi(q)|\,[\hat{R}^{(+)}_s, \hat{Q}(q)]\,|\phi(q)\rangle = \kappa_s(R^{(+)}_s, Q(q)), \tag{3·30}$$

$$f_{N,\tau} \equiv B(q)\frac{\partial\lambda_\tau}{\partial q}. \tag{3·31}$$

Here we have introduced the notation

$$\hat{R}^{(\pm)}_s \equiv [\hat{F}^{(\pm)}_{B,s}, (\hat{h}(q) - \sum_\tau \lambda_\tau(q)\hat{N}_\tau)_A] \equiv \sum_{\mu\bar{\nu}} R^{(\pm)}_s(\mu\bar{\nu})\Big(\boldsymbol{A}^\dagger_{\mu\bar{\nu}}(q) \mp \boldsymbol{A}_{\mu\bar{\nu}}(q)\Big), \tag{3·32}$$

where $(\hat{h}(q)-\sum_\tau \lambda_\tau(q)\hat{N}_\tau)_A$ represents the $\boldsymbol{A}^\dagger_{\mu\bar{\nu}}(q)$ and $\boldsymbol{A}_{\mu\bar{\nu}}(q)$ parts of the operator in parentheses. We also use the notation

$$(F^{(-)}_s, Q(q)) \equiv \sum_{\mu\bar{\nu}} F^{(-)}_s(\mu\bar{\nu})Q_{\mu\bar{\nu}}(q), \quad \text{etc.} \tag{3·33}$$

Note that $f^{(-)}_{Q,s}, f^{(+)}_{P,s}$ and $f^{(+)}_{R,s}$ are linear functions of $Q_{\mu\bar{\nu}}(q)$ or $P_{\mu\bar{\nu}}(q)$.

We can easily derive the following expressions for the matrix elements $Q_{\mu\bar{\nu}}(q)$ and $P_{\mu\bar{\nu}}(q)$ from the local harmonic equations in the moving frame, (3·26) and (3·27):

$$\begin{aligned} Q_{\mu\bar{\nu}}(q) = &\sum_s g_1(\mu\bar{\nu})F^{(-)}_s(\mu\bar{\nu})f^{(-)}_{Q,s} + \sum_s g_2(\mu\bar{\nu})\Big\{F^{(+)}_s(\mu\bar{\nu})f^{(+)}_{PR,s} \\ &+ R^{(-)}_s(\mu\bar{\nu})f^{(-)}_{Q,s} + \sum_\tau N_\tau(\mu\bar{\nu})f_{N,\tau}\Big\} \end{aligned} \tag{3·34}$$

$$\begin{aligned} P_{\mu\bar{\nu}}(q) = &\sum_s g_1(\mu\bar{\nu})\Big\{F^{(+)}_s(\mu\bar{\nu})f^{(+)}_{PR,s} + R^{(-)}_s(\mu\bar{\nu})f^{(-)}_{Q,s} + \sum_\tau N_\tau(\mu\bar{\nu})f_{N,\tau}\Big\} \\ &+ \omega^2(q)\sum_s g_2(\mu\bar{\nu})F^{(-)}_s(\mu\bar{\nu})f^{(-)}_{Q,s}, \end{aligned} \tag{3·35}$$

where $f^{(+)}_{PR,s} = f^{(+)}_{P,s} + f^{(+)}_{R,s}$ and

$$g_1(\mu\bar{\nu}) \equiv \frac{E_\mu + E_{\bar{\nu}}}{(E_\mu + E_{\bar{\nu}})^2 - \omega^2(q)}, \quad g_2(\mu\bar{\nu}) \equiv \frac{1}{(E_\mu + E_{\bar{\nu}})^2 - \omega^2(q)}. \tag{3·36}$$

Note that ω^2, representing the square of the frequency of the local harmonic mode, $\omega(q) = \sqrt{B(q)C(q)}$, is not necessarily positive. The values of $B(q)$ and $C(q)$ depend on the scale of the collective coordinate q, while $\omega(q)$ does not. In other words, the scale of q can be chosen arbitrarily without affecting the frequency $\omega(q)$. We thus require $B(q) = 1$ everywhere on the collective path to uniquely determine the scale of q.

Inserting expressions (3.34) and (3.35) for $Q_{\mu\bar{\nu}}(q)$ and $P_{\mu\bar{\nu}}(q)$ into Eqs. (3.28)-(3.30) and combining them with the condition of orthogonality to the number operators,

$$\langle\phi(q)|[\hat{N}_\tau, \hat{P}(q)]|\phi(q)\rangle = 2i(P(q), N_\tau) = 0, \tag{3·37}$$

we obtain the linear homogeneous equations

$$\sum_{s'\tau'} \begin{pmatrix} S^{Q,Q}_{ss'} & S^{Q,PR}_{ss'} & S^{Q,N}_{s\tau'} \\ S^{PR,Q}_{ss'} & S^{PR,PR}_{ss'} & S^{PR,N}_{s\tau'} \\ S^{N,Q}_{\tau s'} & S^{N,PR}_{\tau s'} & S^{N,N}_{\tau\tau'} \end{pmatrix} \begin{pmatrix} f^{(-)}_{Q,s'} \\ f^{(+)}_{PR,s'} \\ f_{N,\tau'} \end{pmatrix} = 0 \tag{3·38}$$

for the vectors $\boldsymbol{f}_Q^{(-)}$, $\boldsymbol{f}_{PR}^{(+)}$, and $\boldsymbol{f}_N$ defined by

$$\boldsymbol{f}_Q^{(-)} \equiv \{f_{Q,1}^{(-)},\ f_{Q,1}^{(-)}\}, \tag{3·39}$$

$$\boldsymbol{f}_{PR}^{(+)} \equiv \{f_{PR,1}^{(+)},\ f_{PR,2}^{(+)},\ f_{PR,3}^{(+)},\ f_{PR,5}^{(+)}\}, \tag{3·40}$$

$$\boldsymbol{f}_N \equiv \{f_{N,n},\ f_{N,p}\}. \tag{3·41}$$

Here, we have

$$S_{ss'}^{Q,Q} \equiv 2(F_s^{(-)}, F_{s'}^{(-)})_{g_1} + 2(F_s^{(-)}, R_{s'}^{(-)})_{g_2} - \frac{1}{\kappa_s}\delta_{ss'}, \tag{3·42}$$

$$S_{ss'}^{Q,PR} \equiv 2(F_s^{(-)}, F_{s'}^{(+)})_{g_2}, \tag{3·43}$$

$$S_{s\tau'}^{Q,N} \equiv 2(F_s^{(-)}, N_{\tau'})_{g_2}, \tag{3·44}$$

$$\begin{aligned} S_{ss'}^{PR,Q} \equiv{}& 2(F_s^{(+)}, R_{s'}^{(-)})_{g_1} + 2\omega^2(q)(F_s^{(+)}, F_{s'}^{(-)})_{g_2} + (R_s^{(+)}, R_{s'}^{(-)})_{g_2}, \\ &+ (R_s^{(+)}, F_{s'}^{(-)})_{g_1}, \end{aligned} \tag{3·45}$$

$$S_{ss'}^{PR,PR} \equiv 2(F_s^{(+)}, F_{s'}^{(+)})_{g_1} + (R_s^{(+)}, F_{s'}^{(+)})_{g_2} - \frac{1}{\kappa_s}\delta_{ss'}, \tag{3·46}$$

$$S_{s\tau'}^{PR,N} \equiv 2(F_s^{(+)}, N_{\tau'})_{g_1} + (R_s^{(+)}, N_{\tau'})_{g_2}, \tag{3·47}$$

$$S_{\tau s'}^{N,Q} \equiv \omega^2(q)(N_\tau, F_{s'}^{(-)})_{g_2} + (N_\tau, R_{s'}^{(-)})_{g_1}, \tag{3·48}$$

$$S_{\tau s'}^{N,PR} \equiv (N_\tau, F_{s'}^{(+)})_{g_1}, \tag{3·49}$$

$$S_{\tau\tau'}^{N,N} \equiv (N_\tau, N_{\tau'})_{g_1}, \tag{3·50}$$

with the notations

$$(F_s^{(-)}, F_{s'}^{(-)})_{g_1} \equiv \sum_{\mu\bar{\nu}} F_s^{(-)}(\mu\bar{\nu}) g_1(\mu\bar{\nu}) F_{s'}^{(-)}(\mu\bar{\nu}), \quad \text{etc.} \tag{3·51}$$

Equation (3·38) takes the form

$$\sum_{\sigma'=1}^{8} S_{\sigma\sigma'}(\omega^2(q)) f_{\sigma'} = 0 \tag{3·52}$$

for the vector $\boldsymbol{f}$ composed of

$$\{f_{\sigma=1-8}\} \equiv \{\boldsymbol{f}_Q^{(-)},\ \boldsymbol{f}_{PR}^{(+)},\ \boldsymbol{f}_N\} \tag{3·53}$$

$$\equiv \{f_{Q,1}^{(-)},\ f_{Q,2}^{(-)},\ f_{PR,1}^{(+)},\ f_{PR,2}^{(+)},\ f_{PR,3}^{(+)},\ f_{PR,5}^{(+)},\ f_{N,n},\ f_{N,p}\}. \tag{3·54}$$

Thus, the frequency ω of the local harmonic mode is determined by the condition $\det S = 0$. The normalizations of $\boldsymbol{f}$ are fixed by

$$\langle\phi(q)|[\hat{Q}(q), \hat{P}(q)]|\phi(q)\rangle = 2i(Q(q), P(q)) = i. \tag{3·55}$$

Note that ω^2 represents the curvature of the collective potential,

$$\omega^2 = \frac{\partial^2 V}{\partial q^2}, \tag{3·56}$$

for the choice of coordinate scale with which the mass is unity, i.e., $B(q) = 1$.

In concluding this section, we mention that the reduction of the local harmonic equations to linear homogeneous equations like (3·52) can be done for any effective interaction that can be written as a sum of separable terms. Below, we call the local harmonic equations in the moving frame the "moving frame QRPA" for brevity.

§4. Procedure of the calculation

4.1. *Algorithm to find collective paths*

In order to find the collective path connecting the oblate and prolate local minima, we have to determine the state vectors $|\phi(q)\rangle$ and the infinitesimal generators $\hat{Q}(q)$ and $\hat{P}(q)$ by solving the moving frame HB equation (3·14) and the moving frame QRPA equations, (3·26) and (3·27). Because $\hat{Q}(q)$ and $|\phi(q)\rangle$ are mutually dependent, we have to resort to some iterative procedure. We carry this out through the following algorithm.

Let us assume that the state vector $|\phi(q)\rangle$ and the infinitesimal generators $\hat{Q}(q)$ and $\hat{P}(q)$ are known at a specific point of q. We then find the state vector $|\phi(q+\delta q)\rangle$ and the infinitesimal generators $\hat{Q}(q+\delta q)$ and $\hat{P}(q+\delta q)$ at a neighboring point $q+\delta q$ through the following steps.

Step 1: Construct a state vector at the neighboring point $q+\delta q$ using $\hat{P}(q)$:

$$|\phi(q+\delta q)\rangle^{(0)} = e^{-i\delta q\hat{P}(q)}|\phi(q)\rangle. \tag{4·1}$$

Though $|\phi(q+\delta q)\rangle^{(0)}$ does not necessarily satisfy the moving frame HB equation, (3·14), we can use this state vector as an initial guess for $q+\delta q$.

Step 2: Solve the moving frame HB equation (3·14) using $\hat{Q}^{(0)}(q+\delta q) = \hat{Q}(q)$ as an initial guess for $\hat{Q}(q+\delta q)$ and obtain an improved state vector $|\phi(q+\delta q)\rangle^{(1)}$. Doing this, we find it important to impose the constraint

$$\langle\phi(q+\delta q)|\hat{Q}(q)|\phi(q+\delta q)\rangle = \delta q \tag{4·2}$$

for the increment δq of the collective coordinate q, together with the constraints

$$\langle\phi(q+\delta q)|\hat{N}_\tau|\phi(q+\delta q)\rangle = N_\tau, \qquad \tau = p, n \tag{4·3}$$

for the proton and neutron numbers ($N_p = Z,\ N_n = N$). The constraint (4·2) is easily derived by combining Eq. (4·1) with the canonical variable condition (2·8). The details of this step are described in Appendix B.

Step 3: Solve the moving frame QRPA equations, (3·26) and (3·27), with the use of $|\phi(q+\delta q)\rangle^{(1)}$ to obtain $\hat{Q}^{(1)}(q+\delta q)$ and $\hat{P}^{(1)}(q+\delta q)$.

Step 4: Return to *Step 2* and solve Eq. (3·14) using $\hat{Q}^{(1)}(q+\delta q)$.

If the iterative procedure, *Steps 2-4*, converges, we obtain self-consistent solutions, $\hat{Q}(q+\delta q)$, $\hat{P}(q+\delta q)$ and $|\phi(q+\delta q)\rangle$, that satisfy Eqs. (3·14), (3·26) and (3·27) simultaneously at $q+\delta q$. Then, we return to *Step 1* to construct an initial guess $|\phi(q+2\delta q)\rangle^{(0)}$ for the next point, $q+2\delta q$, and repeat the above procedure. In this way, we proceed step by step along the collective path.

The above is a brief summary of the basic algorithm. In actual numerical calculations, we start the procedure from one of the HB local minima and choose the lowest frequency QRPA mode as an initial condition for the infinitesimal generators $\hat{Q}$ and $\hat{P}$ at $q=0$. Under ordinary conditions, we can proceed along the collective path following the procedure described above. In some special situations, however, we need additional considerations concerning the choice of the initial guess, $\hat{Q}^{(0)}(q+\delta q)$, in *Step 2*. Actually, we encounter such situations in some special regions of the collective path for ^{72}Kr. We give detailed discussion of this point in §§5.3.

We have checked that the same collective path is obtained by starting from the other local minimum and proceeding in the inverse manner.

4.2. *Details of the calculation*

In the numerical calculation, we use the spherical single-particle energies of the modified oscillator model of Ref. 83), which are listed in Table I, and follow the conventional prescriptions of the P+Q interaction model,[77] except that the pairing and quadrupole interaction strengths, G_τ and χ, are chosen to approximately reproduce the pairing gaps and quadrupole deformations obtained in the Skyrme-HFB calculation carried out by Yamagami *et al.*[82] The values they obtained are $G_n = 0.320$ (0.299) $G_p = 0.320$ (0.309) and $\chi' \equiv \chi b^4 = 0.248$ (0.255) in units of MeV for ^{68}Se (^{72}Kr), where b is the length parameter given by $b^2 = \frac{4}{5}\left(\frac{2}{3}\right)^{1/3} r_0^2 A^{1/3}$. The pairing gaps, $\Delta_{\tau=p,n}$, and deformation parameters, β and γ, are defined as usual through the expectation values of the pairing and quadrupole operators:

$$\Delta_\tau(q) = G_\tau \langle\phi(q)| \sum_{k\in\tau} d_k^\dagger d_{\bar{k}}^\dagger |\phi(q)\rangle, \tag{4·4}$$

$$\beta\cos\gamma = \chi' \langle\phi(q)|\hat{D}_{20}^{(+)}|\phi(q)\rangle/(\hbar\omega_0 b^2), \tag{4·5}$$

$$\beta\sin\gamma = \sqrt{2}\chi' \langle\phi(q)|\hat{D}_{22}^{(+)}|\phi(q)\rangle/(\hbar\omega_0 b^2). \tag{4·6}$$

Here, $\hbar\omega_0$ denotes the frequency of the harmonic oscillator potential.

Table I. Spherical single-particle orbits and their energies used in the calculation. The energies relative to those of $1g_{9/2}$ are given in units of MeV.

orbits	$1f_{7/2}$	$2p_{3/2}$	$1f_{5/2}$	$2p_{1/2}$	$1g_{9/2}$	$2d_{5/2}$	$1g_{7/2}$	$3s_{1/2}$	$2d_{3/2}$
protons	-8.77	-4.23	-2.41	-1.50	0.0	6.55	5.90	10.10	9.83
neutrons	-9.02	-4.93	-2.66	-2.21	0.0	5.27	6.36	8.34	8.80

§5. Results of the calculation

5.1. *Properties of the QRPA modes at the local minima in ^{68}Se and ^{72}Kr*

For the P+Q Hamiltonian described in §4, the lowest HB solution corresponds to a oblate shape, while the second lowest HB solution possesses a prolate shape for both ^{68}Se and ^{72}Kr (see Table II). Their energy differences are 0.30 and 0.82 MeV for ^{68}Se and ^{72}Kr, respectively. In the QRPA calculations at these local minima, we obtain strongly collective quadrupole modes with low frequencies. They correspond to the β and γ vibrations in deformed nuclei with axial symmetry. Although the former in fact contains pairing vibrational components, we call it a β vibration, because the transition matrix elements for the quadrupole operator $D_{20}^{(+)}$ are enhanced. (A neutron pairing vibrational mode appears as the second QRPA mode at the oblate minimum in ^{72}Kr; see Table II.) We note that there is an important difference between ^{68}Se and ^{72}Kr concerning the relative excitation energies of the β and γ vibrational modes: In the case of ^{68}Se, the frequencies of the γ vibrational QRPA mode are lower than those of the β vibrational one for both the oblate and prolate local minima. The situation is opposite in the case of ^{72}Kr; that is, the frequencies of the β vibrations are lower than those of the γ vibrations. As we see in the succeeding subsections, this difference leads to an important difference in the properties of the collective path connecting the two local minima.

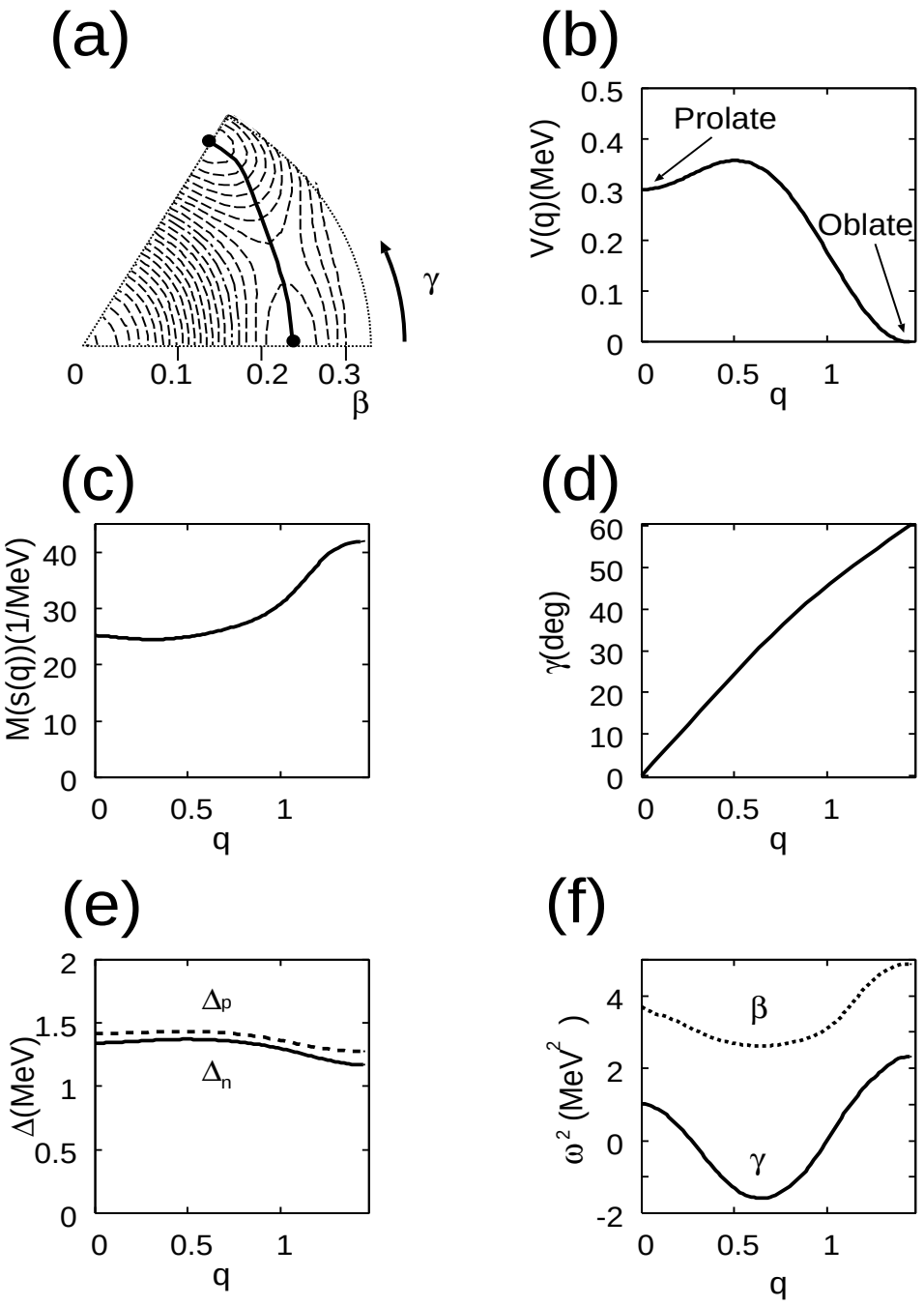

Fig. 1. Results of the calculation for ^{68}Se. (a) The bold curve represents the ASCC path projected onto the (β, γ) plane, which connects the oblate and the prolate minima designated by filled circles. The contour lines were calculated using the conventional constrained HB method and plotted at intervals of 50 keV. (b) Collective potential $V(q)$ plotted as a function of the collective coordinate q. Here the origin of q is chosen to coincide with the prolate local minimum, and its scale is defined such that the collective mass is given by $M(q) = 1$. (c) Collective mass $M(s(q))$ with respect to the geometrical length $s(q)$ along the collective path in the (β, γ)-plane, plotted as a function of q. (d) The triaxiality parameter γ as a function of q. (e) Neutron and proton pairing gaps, Δ_n and Δ_p, as functions of q. (f) The lowest two eigen-frequencies squared (i.e., $\omega^2 = BC$) of the moving frame RPA, plotted as functions of q. These modes at triaxial deformed shapes are more general than the ordinary β- and γ-vibrations in the oblate and prolate limits and contain both components. The symbols β and γ are used, however, to indicate the major components of the moving frame RPA modes.

Table II. The equilibrium quadrupole deformation parameters (β, γ), the pairing gaps (Δ_τ) in units of MeV, the QRPA eigenenergies $\hbar\omega_{\rho=1,2}$ in units of MeV, and the relevant quadrupole transition matrix elements squared, $|M_\rho|^2 \equiv |\langle\rho|D^{(+)}_{2K}|0\rangle|^2$ ($\rho = 1, 2$). Here, $|\rho\rangle$ and $|0\rangle$ denote the QRPA one-phonon and the ground states. The symbols β, γ, and Δ_n in the eighth column respectively indicate the β-, γ- and neutron-pairing vibrational modes; the $|M_\rho|^2$ values for $K = 0,\ 2$ and 0 are presented in Weisskopf units.

	β	γ	Δ_n	Δ_p	ω_1	$\lvert M_1\rvert^2$	ω_2	$\lvert M_2\rvert^2$
^{68}Se (prolate)	0.234	0°	1.34	1.42	1.02(γ)	33.66	1.91(β)	12.19
^{68}Se (oblate)	0.284	60°	1.17	1.27	1.55(γ)	13.64	2.25(β)	7.67
^{72}Kr (prolate)	0.376	0°	1.15	1.29	1.60(β)	12.97	1.67(γ)	14.61
^{72}Kr (oblate)	0.354	60°	0.86	1.00	1.15(β)	5.37	1.91(Δ_n)	0.19

5.2. *Collective path connecting the oblate and prolate minima in ^{68}Se*

As the γ vibrational mode is the lowest frequency and most collective QRPA mode at the prolate local minimum, we have chosen this mode as the initial condition for solving the basic equations of the ASCC method and carried out the procedure described in §§ 4.1. We thus obtained the collective path connecting the oblate and prolate local minima in ^{68}Se, which is plotted in Fig. 1(a). As we have extracted the collective path in the TDHB phase space, which has a very large number of degrees of freedom, the path drawn in this figure should be regarded as a projection of the collective path onto the (β, γ)-plane. Roughly speaking, the collective path goes through the valley that exists in the γ direction and connects the oblate and prolate minima. If β is treated as a collective coordinate and the oblate and prolate shapes are connected through the spherical point, the variation of the potential energy would be much greater than that along the collective path we obtained. The potential energy curve $V(q)$ along the collective path evaluated using the ASCC method is displayed in Fig. 1(b). Because we have defined the scale of the collective coordinate q such that the collective mass is given by $M(q) = B(q)^{-1} = 1\ \mathrm{MeV}^{-1}$, the collective mass as a function of the geometrical length s along the collective path in the (β, γ) plane can be defined by

$$M(s(q)) = M(q)\Big(\frac{ds}{dq}\Big)^{-2}, \tag{5·1}$$

with $ds^2 = d\beta^2 + \beta^2 d\gamma^2$. This quantity is presented in Fig. 1(c) as a function of q. The triaxial deformation parameter γ is plotted as a function of q in Fig. 1(d). Variations of the pairing gaps, $\Delta_\tau(q)$, and of the eigen-frequencies of the moving frame QRPA equations along the collective path are plotted in Figs. 1(e) and (f). The solid curve in Fig. 1(f) represents the frequencies squared, $\omega^2(q) = B(q)C(q)$, given by the product of the inverse mass $B(q)$ and the local stiffness $C(q)$ of the solutions of the moving frame QRPA equations, which correspond to the γ-vibration in the oblate and prolate limits. These QRPA solutions determine the infinitesimal generators $\hat{Q}(q)$ and $\hat{P}(q)$ along the collective path. For reference, we also present in Fig. 1(f) another solution of the moving frame QRPA equations, which possesses the β-vibrational properties and is irrelevant to the collective path in the case of ^{68}Se. Note that the frequency of the γ-vibrational mode becomes imaginary in the region $12° < \gamma < 45°$. These results should reveal interesting dynamical properties of the shape coexistence phenomena in ^{68}Se. For instance, the large collective mass in the vicinity of $\gamma = 60°$ [Fig. 1(c)] might increase the stability of the oblate shape in the ground state. A detailed investigation of these quantities as well as solutions

of the collective Schrödinger equation will be given in a succeeding paper.[84)]

5.3. *Collective path connecting the oblate and prolate minima in ^{72}Kr*

In contrast to ^{68}Se, the lowest-frequency QRPA mode is the β vibration at the prolate local minimum in ^{72}Kr. For this reason, we have chosen this mode as the initial condition at the prolate minimum and started the procedure of extracting the collective path. Then, the collective path first goes in the direction of the β axis in the (β, γ)-plane. As we go along the β axis, we eventually encounter a situation in which the two solutions of the moving frame QRPA equations compete in energy, and they eventually cross. Thus, we see that the properties of the solution with the lowest value of $\omega^2 = BC$ change from those of the β vibrational to those of the γ vibrational case at some point on the collective path. If only the solution $\hat{Q}_1(q)$ with the lowest value of ω^2 at the previous point q is always chosen as an initial guess for $\hat{Q}(q+\delta q)$ in *Step 2* of the algorithm described in §§4.1, then the direction of the collective path in the (β, γ) plane changes abruptly from the β direction to the γ direction immediately after the crossing point (in the vicinity of the point C' in Fig. 3 presented below), and the numerical algorithm outlined in §§4.1 fails at this point: During the iterative procedure of solving the moving frame HB equation, we encounter a situation in which the overlap $(Q(q), Q(q+\delta q))$ between the infinitesimal generators $\hat{Q}$ at the neighboring points q and $q+\delta q$ vanishes, because K=0 for the former, whereas K=2 for the latter. The numerical algorithm (whose details are described in Appendix B) then is no longer effective at this point, where the overlaps $(N_\tau, Q(q+\delta q))$ also vanish for the same reason. This problem exists even if we decrease the step size δq. We find, however, that we can avoid this difficulty by employing a more suitable initial guess for $\hat{Q}(q+\delta q)$. Specifically, we take a linear combination of the two solutions $\hat{Q}_1(q)$ and $\hat{Q}_2(q)$ at the previous point q, $\hat{Q}^{(0)}(q+\delta q) = (1-\varepsilon)\hat{Q}_1(q) + \varepsilon\hat{Q}_2(q)$, with a small coefficient ε, as an initial guess. This improvement is just for the purpose of starting the iterative procedure at the next point, $q+\delta q$, on the collective path, so that the self-consistent solution, $\hat{Q}(q+\delta q)$, obtained upon the convergence of the iterative procedure, of course, does not depend on the values of ε. For instance, we obtain an axially symmetric solution $|\phi(q+\delta q)\rangle$ and a generator $\hat{Q}(q+\delta q)$ preserving the K quantum number in the region satisfying $\beta > 0.24$ around the prolate minimum, even when we start the iterative procedure using an initial guess for $\hat{Q}(q+\delta q)$ that breaks the axial symmetry. We confirmed that this is indeed the case as long as ε is a small finite value around 0.1. This special care is needed only near such crossing points (as shown below in Figs. 3-5), where two solutions of the moving frame QRPA equations with different K quantum numbers compete in energy.

With the improved algorithm mentioned above, we have successfully obtained the smooth deviation of the direction of the collective path from the β axis toward the γ direction [see Fig. 2(a)]. We note that the properties of the lowest ω^2 solution of the local harmonic equations also gradually change from those of the β vibrational to those of the γ vibrational case [see Fig. 2(f)]. The details of the turnover region are presented in Fig. 3. It can clearly be seen in Fig. 3(a) that there is a gradual onset of axial-symmetry breaking in the solutions $|\phi(q)\rangle$ of the moving frame HB equation. It can also be seen in Fig. 3(b) that there is an avoided crossing between the lowest two solutions of the moving frame QRPA equations associated with mixing of the components with K=0 and 2. After a smooth turn in the γ direction, the γ value increases, with the value of β roughly constant, and the collective path eventually

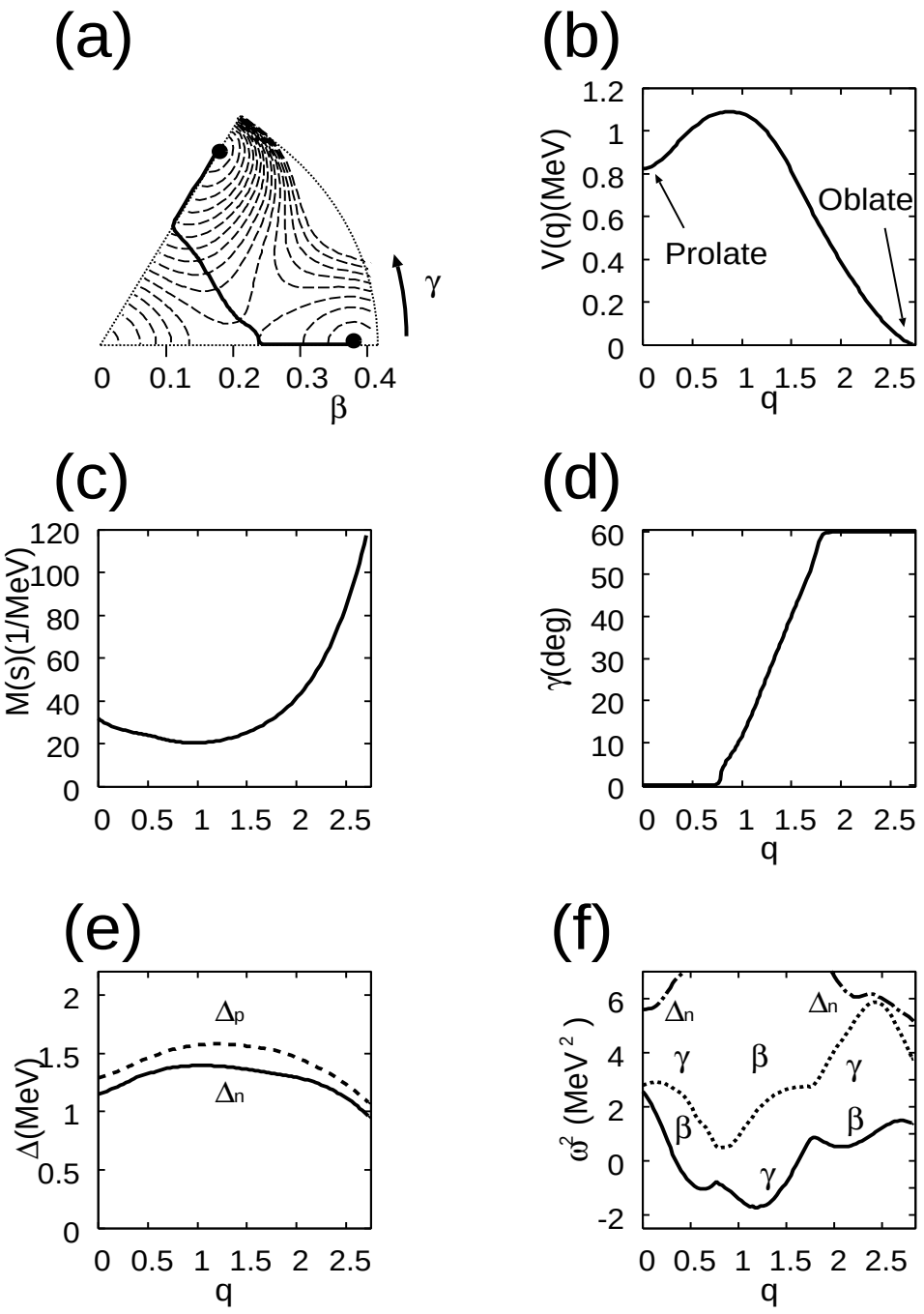

Fig. 2. Results of the calculation for ^{72}Kr. The details here are the same as in Fig. 1, except for the following: In (a), the contour lines are plotted at intervals of 100 keV. In (f), the lowest three eigen-frequencies squared (i.e., $\omega^2 = BC$) of the moving frame RPA are plotted as functions of q. As mentioned in the caption to Fig. 1, these modes at triaxial deformed shapes are more general than the ordinary β- and γ-vibrations in the oblate and prolate limits and contain both components. The symbols β and γ are used, however, in order to indicate the major components of the moving frame RPA modes. Similarly, the symbol Δ_n is used to indicate that the major component is the neutron pairing vibrational mode.

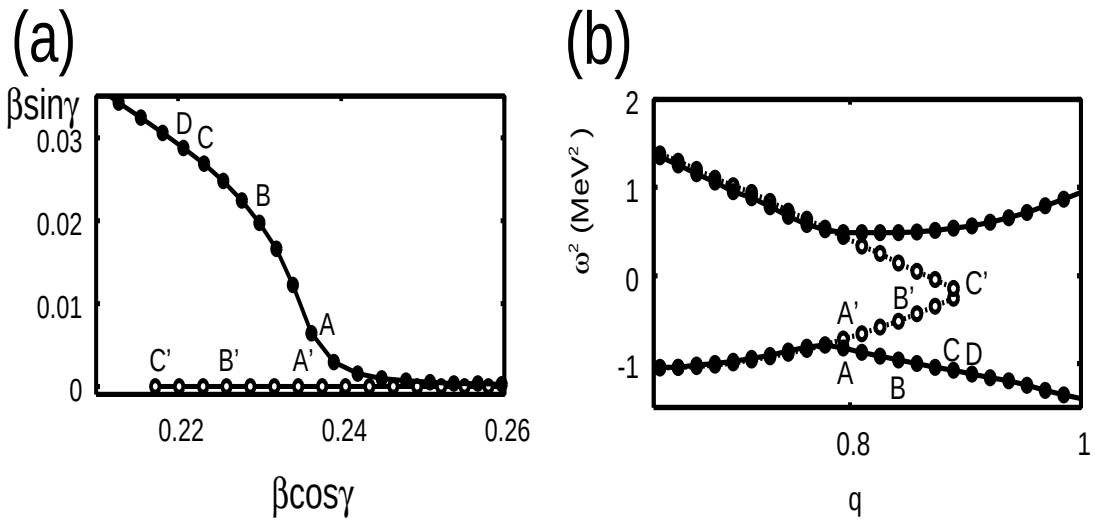

Fig. 3. Enlargement of the turnover region of Figs. 2(a) and (f) for ^{72}Kr, where the collective path turns in the γ direction. A step size $\delta q = 0.0157$ and the value $\varepsilon = 0.1$ were used in the numerical calculation. Every step δq is represented by a filled circle and connected by a solid curve. The points designated A, B, C, D on the collective path in (a) correspond to those in (b), which displays the squared frequencies, ω^2, of the lowest two solutions of the moving frame QRPA equations as functions of the collective coordinate q. The open circles represent those obtained in the calculation with $\varepsilon = 0$, where the mixing effects between the K=0 and 2 components are ignored. The points designated A', B', C' in the latter calculation correspond to the points A, B, C in the former calculation. In the latter calculation, we could not obtain the point corresponding to D, because the problem discussed in the main text is encountered in the numerical algorithm. It was checked that the same collective path is obtained with use of $\delta q = 0.0314$, except that the distances between the successive points are doubled.

approaches the $\gamma = 60^\circ$ axis. Then, we again encounter a similar situation. Adopting the improved algorithm, we have confirmed that the properties of the lowest ω^2 solution change smoothly this time, from those of the γ vibrational to those of the β vibrational case. The collective path thus merges with the $\gamma = 60^\circ$ axis, and it finally reaches the oblate minimum.

We have also carried out a calculation starting from the oblate minimum and proceeded in the inverse manner, obtaining the same collective path. This should be regarded as a crucial test of the consistency of our calculation. Figure 4 presents the details of this test: The collective path that started from the prolate minimum and turned in the γ direction gradually merges with the $\gamma = 60^\circ$ axis. Moving in the opposite direction, we see a gradual onset of axial symmetry breaking in the collective path that started from the oblate minimum. We see that the two results of the calculation for the collective path agree nicely. The importance of taking account of the mixing between the β- and γ-vibrational degrees of freedom in solving the moving frame HB and QRPA equations is again demonstrated in Fig. 5, which displays the details of the turnover region from the $\gamma = 60^\circ$ axis.

Although the collective path plotted in Fig. 2(a) should be regarded as its projection onto the (β, γ)-plane, the result of calculation indicates that the collective path runs roughly along the valley in this plane. The potential energy curve $V(q)$,

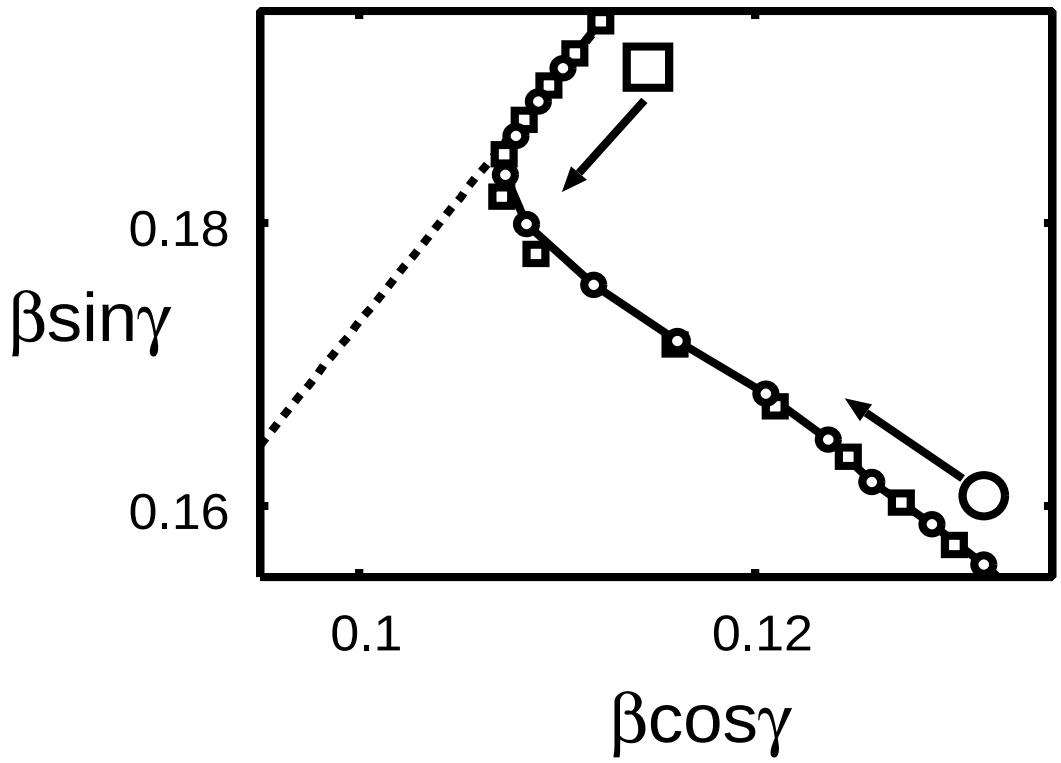

Fig. 4. Enlargement of the turnover region of Figs. 2(a) for ^{72}Kr, where the collective path (solid curve) coming from the prolate minimum merges with the $\gamma = 60^\circ$ axis (dotted line). Every step δq is represented by an open circle and connected by a solid curve. For comparison, the result of calculation starting from the oblate minimum and moving in the opposite direction is represented by open squares. Slight deviations from the solid curve indicate the degree of precision of the present numerical calculation. The step size $\delta q = 0.0157$ and the value $\varepsilon = 0.1$ were used in both cases. The collective path obtained with these different calculations agree well.

the collective mass $M(s(q))$, and the variations of the pairing gaps, $\Delta_\tau(q)$, are presented in Figs. 2(b), (c) and (e), respectively. Their properties are similar to those for ^{68}Se. In particular, we notice again a significant increase of $M(s(q))$ in the vicinity of the oblate minimum.

Quite recently, Almehed and Walet studied the oblate-prolate shape coexistence phenomenon in ^{72}Kr by means of an approach similar to the ASCC method but with some additional approximations[80] and found a collective path going from the oblate minimum over a spherical energy maximum into the prolate secondary minimum. We have also obtained such a collective path when we impose axial symmetry on the solutions $|\phi(q)\rangle$ of the moving frame HB equation and always use only K=0 solutions of the moving frame QRPA equations. However, when we relax such symmetry restrictions and follow the lowest ω^2 solution of the moving frame QRPA equations, we obtain the collective path presented in Fig. 2, which breaks the axial symmetry. The reason for this disagreement is not clear at present. With the parameter values they used for the P+Q Hamiltonian, they did not encounter the change in properties of the lowest moving-frame-QRPA mode on the collective path from those of the β vibrational to those of the γ vibrational case. However, it is interesting that they in fact encountered the avoided crossing with a γ-vibrational mode, similar to the one shown in Fig. 2(f), and obtained a collective path that turns into the triaxial plane

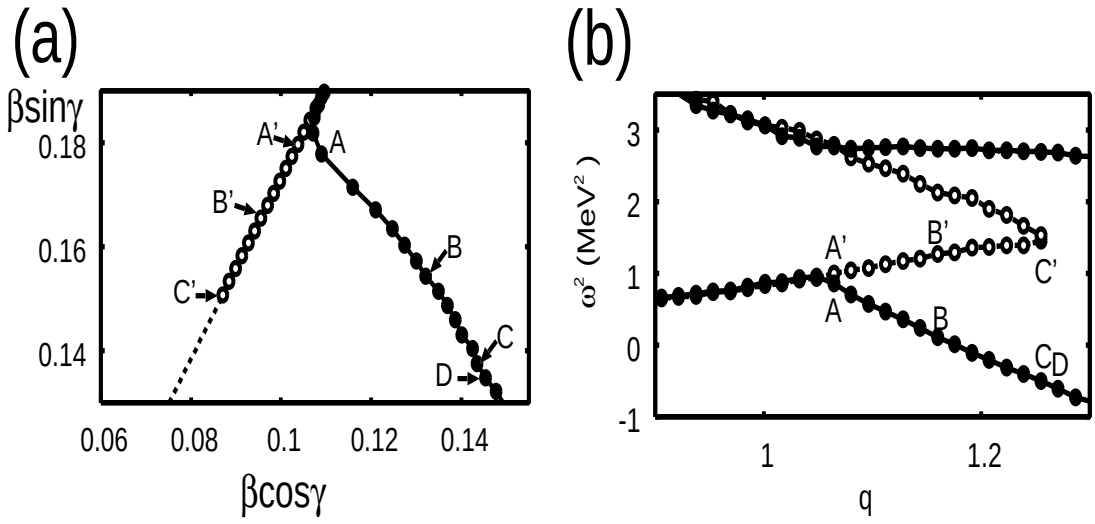

Fig. 5. Enlargement of the turnover region of Figs. 2(a) and (f) for ^{72}Kr, where the collective path (solid curve) coming from the oblate minimum starts to deviate from the $\gamma = 60^\circ$ axis (dotted line). The numerical calculation was done starting from the oblate minimum and using the step size $\delta q = 0.0157$ and the value $\varepsilon = 0.1$. Every step δq is represented by a filled circle and connected by a solid curve. The points designated A, B, C, D on the collective path in (a) correspond to those in (b), which displays the squared frequencies, ω^2, of the lowest two solutions of the moving frame QRPA equations as functions of the collective coordinate q. Note that the values of q in this figure are measured from the oblate minimum. The open circles represent those obtained in the calculation with $\varepsilon = 0$, where the mixing effects between the K=0 and 2 components are ignored. The points designated A', B', C' in the latter calculation correspond to the points A, B, C in the former calculation. In the latter calculation, we cannot get the point corresponding to D, because the problem discussed in the main text is encountered in the numerical algorithm. The slight wiggles along the successive points seen in (b) are due to numerical error, and they indicate the degree of precision of the present numerical calculation. It was checked that the same collective path is obtained with use of $\delta q = 0.0314$, except that the distances between the successive points are doubled.

in their calculation for states with angular momentum $I = 2$.

§6. Concluding remarks

We have applied the ASCC method to the oblate-prolate shape coexistence phenomena in ^{68}Se and ^{72}Kr. It was found that the self-consistent collective paths run approximately along the valley connecting the oblate and prolate local minima in the collective potential energy landscape. This is the first time that the self-consistent collective paths between the oblate and prolate minima have been obtained in realistic situations starting from the microscopic P+Q Hamiltonian. Recently, the generator coordinate method has been used in a number of cases to describe a variety of shape coexistence phenomena, with β employed as the generator coordinate.[47),48)] The triaxial shape vibrational degrees of freedom were also ignored in the extensive variational calculations by the Tübingen group.[49),50)] The result of the ASCC calculation, however, strongly indicates the necessity of taking into account the γ

degree of freedom, at least for the purpose of describing the oblate-prolate shape coexistence in ^{68}Se and ^{72}Kr. In order to evaluate the mixing effects between the oblate and prolate shapes, taking into account the triaxial deformation dynamics, we have to quantize the classical collective Hamiltonian obtained in this paper and solve the resulting collective Schrödinger equation. This will be the subject of a subsequent paper.[84)]

Acknowledgements

This work was done as a part of the Japan-U.S. Cooperative Science Program "Mean-Field Approach to Collective Excitations in Unstable Medium-Mass and Heavy Nuclei", and is supported by a Grant-in-Aid for the 21st Century COE "Center for Diversity and Universality in Physics" from the Ministry of Education, Culture, Sports, Science and Technology (MEXT) of Japan and also by Grants-in-Aid for Scientific Research (Nos. 14540250 and 14740146) from the Japan Society for the Promotion of Science. The numerical calculations were performed on the NEC SX-5 supercomputer at Yukawa Institute for Theoretical Physics, Kyoto University.

Appendix A
—— *Explicit Expressions of the Quasiparticle Matrix Elements* ——

Combining the successive Bogoliubov transformations, (3.8) and (3.18), the quasiparticles, $a^\dagger_\mu(q)$ and $a_\mu(q)$, associated with the state $|\phi(q)\rangle$, can be written in terms of the nucleon operator, $d^\dagger_k$ and $d_{\bar{k}}$, as

$$\begin{pmatrix} a^\dagger_\mu(q) \\ a_{\bar{\mu}}(q) \end{pmatrix} = \sum_k \begin{pmatrix} U_{\mu k}(q) & V_{\mu\bar{k}}(q) \\ V_{\bar{\mu}k}(q) & U_{\bar{\mu}\bar{k}}(q) \end{pmatrix} \begin{pmatrix} d^\dagger_k \\ d_{\bar{k}} \end{pmatrix} \tag{A·1}$$

Making use of the inverse transformation,

$$\begin{pmatrix} d^\dagger_k \\ d_{\bar{k}} \end{pmatrix} = \sum_\mu \begin{pmatrix} U_{k\mu}(q) & V_{k\bar{\mu}}(q) \\ V_{\bar{k}\mu}(q) & U_{\bar{k}\bar{\mu}}(q) \end{pmatrix} \begin{pmatrix} a^\dagger_\mu(q) \\ a_{\bar{\mu}}(q) \end{pmatrix}, \tag{A·2}$$

one can easily derive explicit expressions for the expectation values and the matrix elements of the operators $\hat{F}^{(\pm)}_s$ appearing in Eq. (3·22):

$$\begin{aligned}
\langle\phi(q)|\,\hat{F}^{(+)}_{s=1,2}\,|\phi(q)\rangle &= -2\sum_\mu\sum_k (k\bar{k}|A^{(+)}_{\tau=n,p}|0)U_{k\mu}(q)V_{\bar{k}\mu}(q), \\
F^{(\pm)}_{s=1,2}(\mu\bar{\nu}) &= \sum_k (k\bar{k}|A^{(\pm)}_{\tau=n,p}|0)\Big(U_{k\mu}(q)U_{\bar{k}\bar{\nu}}(q) \pm V_{k\bar{\nu}}(q)V_{\bar{k}\mu}(q)\Big), \\
F^{(\pm)}_{B,s=1,2}(\mu\nu) &= \sum_k (k\bar{k}|A^{(\pm)}_{\tau=n,p}|0)\Big(U_{k\mu}(q)V_{\bar{k}\nu}(q) \pm U_{k\nu}(q)V_{\bar{k}\mu}(q)\Big), \\
\langle\phi(q)|\,\hat{F}^{(+)}_{s=3,5}\,|\phi(q)\rangle &= 2\sum_{\bar{\mu}}\sum_{kl} (k|D^{(+)}_{2,K=0,2}|l)V_{k\bar{\mu}}(q)V_{l\bar{\mu}}(q), \\
F^{(+)}_{s=3,5}(\mu\bar{\nu}) &= \sum_{kl} (k|D^{(+)}_{2,K=0,2}|l)\Big(U_{k\mu}(q)V_{l\bar{\nu}}(q) + U_{k\nu}(q)V_{l\bar{\mu}}(q)\Big), \\
F^{(+)}_{B,s=3,5}(\mu\nu) &= \sum_{kl} (k|D^{(+)}_{2,K=0,2}|l)\Big(U_{k\mu}(q)U_{l\nu}(q) - V_{k\bar{\nu}}(q)V_{l\bar{\mu}}(q)\Big).
\end{aligned} \tag{A·3}$$

The expectation values of the anti-Hermitian operators $A^{(-)}_{\tau=n,p}$ vanish. The quantities $(k|D^{(+)}_{2K}|l)$, etc., appearing in the above expressions are the matrix elements between the single-particle states defined by Eq. (3·5):

$$\begin{aligned}(k|D^{(+)}_{2K}|l) &\equiv (0|d_k D^{(+)}_{2K} d^\dagger_l|0),\\ (k\bar{k}|A^{(\pm)}_\tau|0) &\equiv (0|d_{\bar{k}} d_k A^{(\pm)}_\tau|0), \quad \text{etc.},\end{aligned} \tag{A·4}$$

where $|0)$ is the vacuum for the nucleon operators $(d^\dagger, d)$. The matrix elements of the Bogoliubov transformations, (A.1) and (A.2), possess the following symmetries:

$$U_{\mu k} = U_{\bar{\mu}\bar{k}} = U_{k\mu} = U_{\bar{k}\bar{\mu}}, \quad V_{\mu\bar{k}} = -V_{\bar{\mu}k} = V_{k\bar{\mu}} = -V_{\bar{k}\mu}. \tag{A·5}$$

It is also easily seen that equalities

$$(\bar{k}|D^{(+)}_{2,K=0,2}|\bar{l}) = (k|D^{(+)}_{2,K=0,2}|l), \tag{A·6}$$

$$F^{(\pm)}_{B,s}(\bar{\mu}\bar{\nu}) = F^{(\pm)}_{B,s}(\mu\nu), \quad F^{(\pm)}_{B,s}(\nu\mu) = \pm F^{(\pm)}_{B,s}(\mu\nu) \tag{A·7}$$

hold for the pairing and quadrupole operators under consideration $\{A^{(\pm)}_n, A^{(\pm)}_p, D^{(+)}_{20}, D^{(+)}_{22}\}$. The expectation values $\langle\phi(q)|\,\hat{N}_\tau\,|\phi(q)\rangle$ and the matrix elements $N_\tau(\mu)$ and $N_{B,\tau}(\mu)$ of the neutron and proton number operators are readily obtained from those of $\hat{F}^{(+)}_{s=3}$ by replacing $(k|D^{(+)}_{20}|l)$ with δ_{kl} and restricting the sum over the single-particle index k to neutrons or protons.

Appendix B
—— *Solving the Moving Frame HB Equation* ——

We solve the moving frame HB equation using a method similar to the imaginary time method.[85] Let $\left|\phi^{(i)}(q)\right\rangle$ be the state vector at the iterative step i. We first calculate the mean-field Hamiltonian associate with it:

$$\begin{aligned}\hat{h}^{(i)}(q) &= \sum_k \epsilon_k (d^\dagger_k d_k + d^\dagger_{\bar{k}} d_{\bar{k}}) - \sum_s \kappa_s \langle \hat{F}^{(+)}_s \rangle^{(i)} \hat{F}^{(+)}_s,\\ \langle \hat{F}^{(+)}_s \rangle^{(i)} &\equiv \left\langle \phi^{(i)}(q) \right| \hat{F}^{(+)}_s \left| \phi^{(i)}(q) \right\rangle .\end{aligned} \tag{B·1}$$

Using the quasiparticle operators $b^{(i)\dagger}_\mu$ and $b^{(i)}_\mu$ defined by

$$b^{(i)}_\mu \left|\phi^{(i)}(q)\right\rangle = 0, \tag{B·2}$$

we then generate the state vector at the $(i+1)$th step as

$$\begin{aligned}\left|\phi^{(i+1)}(q)\right\rangle &\equiv \exp \hat{X}^{(i+1)} \left|\phi^{(i)}(q)\right\rangle\\ \hat{X}^{(i+1)} &= -\varepsilon\Big(\hat{h}^{(i)}(q) - \sum_\tau \lambda^{(i+1)}_\tau(q)\hat{N}_\tau - \mu^{(i+1)}(q)\hat{Q}(q)\Big)_+\\ &\quad + \varepsilon\Big(\hat{h}^{(i)}(q) - \sum_\tau \lambda^{(i+1)}_\tau(q)\hat{N}_\tau - \mu^{(i+1)}(q)\hat{Q}(q)\Big)_-\\ &\equiv \sum_{\mu\bar{\nu}} x^{(i+1)}_{\mu\bar{\nu}} \Big(\boldsymbol{X}^{(i)\dagger}_{\mu\bar{\nu}} - \boldsymbol{X}^{(i)}_{\mu\bar{\nu}}\Big),\end{aligned} \tag{B·3}$$

where ε is a small parameter,

$$\boldsymbol{X}^{(i)\dagger}_{\mu\bar{\nu}} = b^{(i)\dagger}_{\mu} b^{(i)\dagger}_{\bar{\nu}}, \quad \boldsymbol{X}^{(i)}_{\mu\bar{\nu}} = b^{(i)}_{\bar{\nu}} b^{(i)}_{\mu}, \tag{B·4}$$

and the subscripts + and − denote the two-quasiparticle creation and annihilation parts of the operator in the parentheses, respectively. It should be noted that, in contrast to the conventinal imaginary time method, the unitary operator $\exp \hat{X}^{(i+1)}$ is used here so that the normalization is preserved during the iteration. The Lagrange multipliers $\lambda^{(i+1)}_{\tau}(q)$ and $\mu^{(i+1)}(q)$ are determined by the constraint equations

$$\begin{aligned} \left\langle \phi^{(i+1)}(q) \right| \hat{N}_{\tau} \left| \phi^{(i+1)}(q) \right\rangle &= N^{(0)}_{\tau}, \\ \left\langle \phi^{(i+1)}(q) \right| \hat{Q}(q-\delta q) \left| \phi^{(i+1)}(q) \right\rangle &= \delta q, \end{aligned} \tag{B·5}$$

where $N^{(0)}_{n}$ and $N^{(0)}_{p}$ are the neutron and proton numbers of the nucleus under consideration. Similar but slightly different constraints were utilized by Almehed and Walet.[79] Expanding the left-hand sides up to first order in $x^{(i+1)}$, we obtain equations determining them:

$$\begin{aligned} &\begin{pmatrix} (N_n, N_n) & (N_n, N_p) & (N_n, Q(q)) \\ (N_p, N_n) & (N_p, N_p) & (N_p, Q(q)) \\ (Q(q-\delta q), N_n) & (Q(q-\delta q), N_p) & (Q(q-\delta q), Q(q)) \end{pmatrix} \begin{pmatrix} \lambda^{(i+1)}_{n}(q) \\ \lambda^{(i+1)}_{p}(q) \\ \mu^{(i+1)}(q) \end{pmatrix} \\ &\qquad = \begin{pmatrix} (N^{(0)}_{n} - \langle \hat{N}_n \rangle^{(i)})/2\varepsilon + (h^{(i)}(q), N_n) \\ (N^{(0)}_{p} - \langle \hat{N}_p \rangle^{(i)})/2\varepsilon + (h^{(i)}(q), N_p) \\ (\delta q - \langle \hat{Q}(q-\delta q) \rangle^{(i)})/2\varepsilon + (h^{(i)}(q), Q(q-\delta q)), \end{pmatrix} \end{aligned} \tag{B·6}$$

where the quantities $(N_\tau, N_{\tau'}), (N_\tau, Q(q))$, etc., are defined by (3.33), except that the coefficients $N_\tau(\mu), Q_{\mu\bar{\nu}}(q)$, etc., involved in these quantities are here defined with respect to the two-quasiparticle creation and annihilation operators, $\boldsymbol{X}^{(i)\dagger}_{\mu\bar{\nu}}$ and $\boldsymbol{X}^{(i)}_{\mu\bar{\nu}}$. Using the state vector $\left|\phi^{(i+1)}(q)\right\rangle$, we calculate the mean-field Hamiltonian $\hat{h}^{(i+1)}(q)$ at the $(i+1)$th step, and repeat the above procedure until convergence is attained. The mean-field Hamiltonian thus obtained takes the following form:

$$\begin{aligned} \hat{h}_M(q) &= \hat{h}(q) - \sum_{\tau} \lambda_\tau(q) \hat{N}_\tau - \mu(q) \hat{Q}(q) \\ &= \langle \phi(q) | \, \hat{h}_M(q) \, | \phi(q) \rangle + \sum_{\mu\nu} h_{\mu\nu}(q) \Big(b^{\dagger}_{\mu}(q) b_{\nu}(q) + b^{\dagger}_{\bar{\mu}}(q) b_{\bar{\nu}}(q) \Big). \end{aligned} \tag{B·7}$$

Finally we introduce the quasiparticle operators $a^{\dagger}_{\mu}(q)$ and $a_{\mu}(q)$ that diagonalize $\hat{h}_M(q)$:

$$\hat{h}_M(q) = \langle \phi(q) | \, \hat{h}_M(q) \, | \phi(q) \rangle + \sum_{\mu} E_\mu(q) \Big(a^{\dagger}_{\mu}(q) a_{\mu}(q) + a^{\dagger}_{\bar{\mu}}(q) a_{\bar{\mu}}(q) \Big). \tag{B·8}$$

It is easy to see that $\mu(q) = \partial V / \partial q$. In actual calculations, the above procedure is a part of the double iterative algorithm described in §4. Specifically, we carry out the above iterative procedure using the constraint operator $\hat{Q}(q)^{(n)}$ that is obtained in the n-th iteration step determining the infinitesimal generators, $\hat{Q}(p)$ and $\hat{P}(q)$.

References

1) P. Ring and P. Schuck, *The Nuclear Many-Body Problem* (Springer-Verlag, 1980).
2) J.-P. Blaizot and G. Ripka, *Quantum Theory of Finite Systems* (The MIT press, 1986).
3) A. Klein and E. R. Marshalek, Rev. Mod. Phys. **63** (1991), 375.
4) G. Do Dang, A. Klein and N.R. Walet, Phys. Rep. **335** (2000), 93.
5) A. Kuriyama, K. Matsuyanagi, F. Sakata, K. Takada, and M. Yamamura (eds), Prog. Theor. Phys. Suppl. No. 141 (2001).
6) D.J. Rowe and R. Bassermann, Canad. J. Phys. **54** (1976), 1941.
7) K. Goeke, Nucl. Phys. A **265** (1976), 301.
8) F. Villars, Nucl. Phys. A **285** (1977), 269.
9) T. Marumori, Prog. Theor. Phys. **57** (1977), 112.
10) M. Baranger and M. Veneroni, Ann. of Phys. **114** (1978), 123.
11) K. Goeke and P.-G. Reinhard, Ann. of Phys. **112** (1978), 328.
12) T. Marumori, T. Maskawa, F. Sakata and A.Kuriyama, Prog. Theor. Phys. **64** (1980), 1294.
13) M. J. Giannoni and P. Quentin, Phys. Rev. C **21** (1980), 2060.
14) J. Dobaczewski and J. Skalski, Nucl. Phys. A **369** (1981), 123.
15) K. Goeke, P.-G. Reinhard and D.J. Rowe, Nucl. Phys. A **359** (1981), 408.
16) A. K. Mukherjee and M. K. Pal, Phys. Lett. B **100** (1981), 457; Nucl. Phys. A **373** (1982), 289.
17) D. J. Rowe, Nucl. Phys. A **391** (1982), 307.
18) C. Fiolhais and R.M. Dreizler, Nucl. Phys. A **393** (1983), 205.
19) K. Goeke, F. Grümmer and P.-G. Reinhard, Ann. of Phys. **150** (1983), 504.
20) A. Kuriyama and M. Yamamura, Prog. Theor. Phys. **70** (1983), 1675; ibid. **71** (1984), 122.
21) M. Yamamura, A. Kuriyama and S. Iida, Prog. Theor. Phys. **71** (1984), 109.
22) M. Matsuo and K. Matsuyanagi, Prog. Theor. Phys. **74** (1985), 288.
23) M. Matsuo, Prog. Theor. Phys. **76** (1986), 372.
24) Y. R. Shimizu and K. Takada, Prog. Theor. Phys. **77** (1987), 1192.
25) M. Yamamura and A. Kuriyama, Prog. Theor. Phys. Suppl. No. 93 (1987), 1.
26) N. R. Walet, G. Do Dang and A. Klein, Phys. Rev. C **43** (1991), 2254.
27) A. Klein, N. R. Walet and G. Do Dang, Ann. of Phys. **208** (1991), 90.
28) K. Kaneko, Phys. Rev. C **49** (1994), 3014.
29) T. Nakatsukasa and N. R. Walet, Phys. Rev. C **57** (1998), 1192.
30) T. Nakatsukasa and N. R. Walet, Phys. Rev. C **58** (1998), 3397.
31) J. Libert, M. Girod and J.-P. Delaroche, Phys. Rev. C **60** (1999), 054301.
32) E. Kh. Yuldashbaeva, J. Libert, P. Quentin and M. Girod, Phys. Lett. B **461** (1999), 1.
33) T. Nakatsukasa, N. R. Walet and G. Do Dang, Phys. Rev. C **61** (2000), 014302.
34) J.L. Wood, K. Heyde, W. Nazarewicz, M. Huyse and P. van Duppen, Phys. Rep. **215** (1992), 101.
35) W. Nazarewicz, Phys. Lett. B **305** (1993), 195.
36) W. Nazarewicz, Nucl. Phys. A **557** (1993), 489c.
37) N. Tajima, H. Flocard, P. Bonche, J. Dobaczewski and P.-H. Heenen, Nucl. Phys. A **551** (1993), 409.
38) P. Bonche, E. Chabanat, B. Q. Chen, J. Dobaczewski, H. Flocard, B. Gall, P. H. Heenen, J. Meyer, N. Tajima and M. S. Weiss, Nucl. Phys. A **574** (1994), 185c.
39) P.-G. Reinhard, D.J. Dean, W. Nazarewicz, J. Dobaczewski, J. A. Maruhn and M. R. Strayer, Phys. Rev. C **60** (1999), 014316.
40) A. N. Andreyev et al., Nature **405** (2000), 430; Nucl. Phys. A **682** (2001), 482c.
41) S. M. Fischer et al., Phys. Rev. Lett. **84** (2000), 4064; Phys. Rev. C **67** (2003), 064318.
42) E. Bouchez et al., Phys. Rev. Lett. **90** (2003), 082502.
43) R. R. Rodríguez-Guzmán, J. L. Egido and L. M. Robledo, Phys. Rev. C **62** (2000), 054319; ibid. C **65** (2002), 024304 ; ibid. C **69** (2004), 054319.
44) J. L. Egido, and L. M. Robledo and R. R. Rodríguez-Guzmán, Phys. Rev. Lett. **93** (2004), 082502.
45) R. R. Chasman, J. L. Egido and L. M. Robledo, Phys. Lett. B **513** (2001), 325.
46) T. Nikšić, D. Vretenar, P. Ring and G. A. Lalazissis, Phys. Rev. C **65** (2002), 054320.
47) T. Duguet, M. Bender, P. Bonche and P.-H. Heenen, Phys. Lett. B **559** (2003), 201.
48) M. Bender, P. Bonche, T. Duguet and P.-H. Heenen, Phys. Rev. C **69** (2004), 064303.
49) A. Petrovici, K. W. Schmid, A. Faessler, J. H. Hamilton and A. V. Ramayya, Prog. in Part. Nucl. Phys. **43** (1999), 485.
50) A. Petrovici, K. W. Schmid and A. Faessler, Nucl. Phys. A **665** (2000) 333; ibid. **710** (2002), 246.

51) R. Fossion, K. Heyde, G. Thiamova and P. Van Isacker, Phys. Rev. C **67** (2003), 024306.
52) A. Frank, P. Van Isacker, and C.E. Vargas, Phys. Rev. C **69** (2004), 034323.
53) C. D. Dracoulis et al. Phys. Rev. C **69** (2004), 054318.
54) K. Kaneko, M. Hasegawa, and T. Mizusaki, Phys. Rev. C **66** (2002), 051306(R); nucl-th/0410046.
55) M. Hasegawa, K. Kaneko, T. Mizusaki and S. Tazaki, Phys. Rev. C **69** (2004), 034324.
56) M. Hasegawa, K. Kaneko and T. Mizusaki, nucl-th/0408062; nucl-th/0408063.
57) Y. Sun, Eur. Phys. J. A **20** (2004), 133.
58) M. Matsuo, Prog. Theor. Phys. **72** (1984), 666.
59) M. Matsuo and K. Matsuyanagi, Prog. Theor. Phys. **74** (1985), 1227; ibid. **76** (1986), 93; ibid. **78** (1987), 591.
60) M. Matsuo, Y. R. Shimizu and K. Matsuyanagi, *Proceedings of the Niels Bohr Centennial Conf. on Nuclear Structure*, ed. R. Broglia, G. Hagemann and B. Herskind (North-Holland, 1985), p. 161.
61) K. Takada, K. Yamada and H. Tsukuma, Nucl. Phys. A **496** (1989), 224.
62) K. Yamada, K. Takada and H. Tsukuma, Nucl. Phys. A **496** (1989), 239.
63) K. Yamada and K. Takada, Nucl. Phys. A **503** (1989), 53.
64) H. Aiba, Prog. Theor. Phys. **84** (1990), 908.
65) K. Yamada, Prog. Theor. Phys. **85** (1991), 805; ibid. **89** (1993), 995.
66) J. Terasaki, T. Marumori and F. Sakata, Prog. Theor. Phys. **85** (1991), 1235.
67) J. Terasaki, Prog. Theor. Phys. **88** (1992), 529; ibid. **92** (1994), 535.
68) M. Matsuo, in *New Trends in Nuclear Collective Dynamics*, eds. Y. Abe, H. Horiuchi and K. Matsuyanagi, (Springer-Verlag, 1992), p.219.
69) Y. R. Shimizu and K. Matsuyanagi, Prog. Theor. Phys. Suppl. No. 141 (2001), 285.
70) M. Matsuo, T. Nakatsukasa and K. Matsuyanagi, Prog. Theor. Phys. **103** (2000), 959.
71) M. Kobayasi, T. Nakatsukasa, M. Matsuo and K. Matsuyanagi, Prog. Theor. Phys. **110** (2003), 65.
72) K. Matsuyanagi, Prog. Theor. Phys. 67 (1982) 1141; *Proceedings of the Nuclear Physics Workshop, Trieste, 5-30 Oct. 1981.* ed. C.H. Dasso, R.A. Broglia and A. Winther (North-Holland, 1982), p. 29.
73) Y. Mizobuchi, Prog. Theor. Phys. **65** (1981), 1450.
74) T. Suzuki and Y. Mizobuchi, Prog. Theor. Phys. **79** (1988), 480.
75) T. Fukui, M. Matsuo and K. Matsuyanagi, Prog. Theor. Phys. **85** (1991), 281.
76) M. Baranger and K. Kumar, Nucl. Phys. **62** (1965), 113; Nucl. Phys. A **110** (1968), 529; Nucl. Phys. A **122** (1968), 241; Nucl. Phys. A **122** (1968), 273.
77) M. Baranger and K. Kumar, Nucl. Phys. A **110** (1968), 490.
78) D. R. Bes and R. A. Sorensen, *Advances in Nuclear Physics* (Prenum Press, 1969), vol. 2, p. 129.
79) D. Almehed and N. R. Walet, Phys. Rev. C **69** (2004), 024302.
80) D. Almehed and N. R. Walet, Phys. Lett. B **604** (2004), 163.
81) M. Kobayasi, T. Nakatsukasa, M. Matsuo and K. Matsuyanagi, Prog. Theor. Phys. **112** (2004), 363.
82) M. Yamagami, K. Matsuyanagi and M. Matsuo, Nucl. Phys. A **693** (2001), 579.
83) T. Bengtsson and I. Ragnarsson, Nucl. Phys. A **436** (1985), 14.
84) M. Kobayasi, T. Nakatsukasa, M. Matsuo and K. Matsuyanagi, in preparation.
85) K. T. R. Davies, H. Flocard, S. Krieger and M.S. Weiss, Nucl. Phys. A **342** (1980), 111.